J. Fluid Mech. (2004), *vol.* 502, *pp.* 153–174.
DOI: 10.1017/S0022112003007778 Printed in the United Kingdom

Envelope equations for the Rayleigh–Bénard–Poiseuille system. Part 1. Spatially homogeneous case

By PHILIPPE CARRIÈRE[1], PETER A. MONKEWITZ[2] AND DENIS MARTINAND[1,2]†

[1]Laboratoire de Mécanique des Fluides et d'Acoustique, UMR CNRS 5509, Ecole Centrale de Lyon-Université Claude Bernard Lyon I-INSA Lyon BP163, 69131 Ecully cedex, France

[2]Laboratoire de Mécanique des Fluides, Ecole Polytechnique Fédérale de Lausanne, CH-1015, Lausanne, Switzerland

(Received 7 March 2003 and in revised form 21 October 2003)

Envelope equations are derived for the convection rolls in the Rayleigh–Bénard–Poiseuille system, taking into account both their slow streamwise and transverse variations. At finite $O(1)$ Reynolds numbers, the stability of finite-amplitude longitudinal roll patterns is accessible to analysis in a moving frame of reference and stability is predicted provided a generalized Eckhaus criterion is satisfied. At lower Reynolds numbers, the analysis allows the analytical determination of the Green function for arbitrary orientations of the instability pattern. It clarifies previous results concerning the purely convective nature of all modes of instability except transverse rolls (for which a convective–absolute transition exists), as soon as the Reynolds number is non-zero.

1. Introduction

The destabilization of a motionless horizontal fluid layer heated from below, the so-called Rayleigh–Bénard (RB) problem, has received considerable attention in the past century since the original observations of Bénard (1900) and may now be considered well understood. The linear stability analysis of an infinitely extended, uniformly heated layer developed by Rayleigh (1916), generalized to the case of a no-slip condition at the horizontal boundaries by Pellew & Southwell (1940), was always found to give a satisfactory prediction of the critical temperature difference for the appearance of convective cells in large-aspect-ratio containers (see Silveston 1958; Koschmieder & Pallas 1974). An explanation for such an agreement is provided by the coincidence of the threshold for monotonic stability, as predicted by an energy method (Sorokin 1953, 1954; Joseph 1976), with the threshold for linear instability which excludes any kind of subcritical bifurcation. In addition, its absolute nature in the sense of Briggs (1964) ensures that the instability invades the whole fluid layer, once the temperature difference between top and bottom boundary has reached a supercritical value. The question of the convection pattern selection, which remains unanswered at the linear stage, was first explored by means of amplitude

† Present address: Turbulence and Mixing Group, Department of Aeronautics, Imperial College London, London SW7 2BY, UK.

equations, often termed Stuart–Landau equations after the rigorous derivation by Stuart (1960) of the Landau (1944) conjecture in parallel flows. Generalizing the previous work of Malkus & Veronis (1958), Schlüter, Lortz & Busse (1965) showed that the stable roll pattern for convection between rigid walls successfully corresponds to the usually observed pattern, while hexagonal cells or still more exotic patterns may be encountered owing to temperature dependence of the viscosity, for instance, as in Palm (1960) (see White 1988, for experimental evidence of the zoology of possible patterns). In this context, geometrical constraints imposed by the finite extent of the experimental apparatus have a strong influence on the final orientation and the local details of the pattern. Allowing slow spatial variations in the original multiple scale analysis, Newell & Whitehead (1969) and Segel (1969) used the envelope equation formalism to predict the spatial modulation of the amplitude, in particular, the preferential alignment of rolls parallel to the shorter side of a rectangular 'box'.

Considering now cases where a mean shear flow, e.g. a Poiseuille flow in the present paper, is imposed on the differentially heated fluid layer, the destabilization scenario becomes more complicated. The linear stability analysis of Gage & Reid (1968) has shown that the loss of horizontal isotropy induces a dependency of the critical temperature difference, i.e. the critical Rayleigh number $\mathscr{R}_c^{(\varphi)}$, on the roll orientation φ, where φ is the angle between the horizontal wavevector and the streamwise direction. For longitudinal rolls (LR), i.e. rolls with their axes aligned with the streamwise direction, $\mathscr{R}_c^{(\pi/2)}$ is easily found to be independent of the Reynolds number R, characterizing the mean flow, while for any other direction, $\mathscr{R}_c^{(\varphi)}$ is found to be an increasing function of R†. Consequently, longitudinal rolls were always considered to be the preferred pattern in Rayleigh–Bénard–Poiseuille convection (RBP convection) and, indeed, were repeatedly observed in early experiments (Akiyama, Hwang & Cheng 1971; Ostrach & Kamotani 1975; Fukui, Nakajima & Hueda 1983). However, the existence of travelling transverse roll (TR) convection in some regions of the $\mathscr{R}$–R parameter space is now well established experimentally (Luijkx, Platten & Legros 1981; Ouazzani *et al.* 1989; 1990, 1995; Schröder & Bühler 1995; Yu *et al.* 1997; Chang, Yu & Lin 1997). This pattern has also been obtained from 'direct' numerical simulations of the full set of incompressible Navier–Stokes equations under the usual Boussinesq approximations (see, for instance, Schröder & Bühler 1995; Chen & Lavine 1996). TR convection is thus a possible state of the RBP system, but it is not obvious why it can appear in spite of the lower instability threshold of LR convection. It seems that TRs are preferentially observed at low values of R (on which this paper will concentrate).

To illustrate the added difficulties of the RBP problem as compared to the pure Rayleigh–Bénard case, we have to go a step beyond the linear stability analysis. Following the original work of Richter (1973), Kelly (1994) proposed modeling the problem by means of two real amplitude equations of the kind:

$$\frac{\mathrm{d}A_\perp}{\mathrm{d}t} = (r-\rho^2)A_\perp - A_\perp^3 - (1+\beta^2)A_\perp A_\parallel^2, \tag{1.1a}$$

$$\frac{\mathrm{d}A_\parallel}{\mathrm{d}t} = rA_\parallel - A_\parallel^3 - (1+\beta^2)A_\parallel A_\perp^2, \tag{1.1b}$$

† Strictly speaking, the analysis of Gage & Reid (1968) is only valid when the Prandtl number is unity. Later studies suggested that the results are relevant for arbitrary Prandtl numbers, see for instance Müller (1990); Müller, Lücke & Kamps (1992).

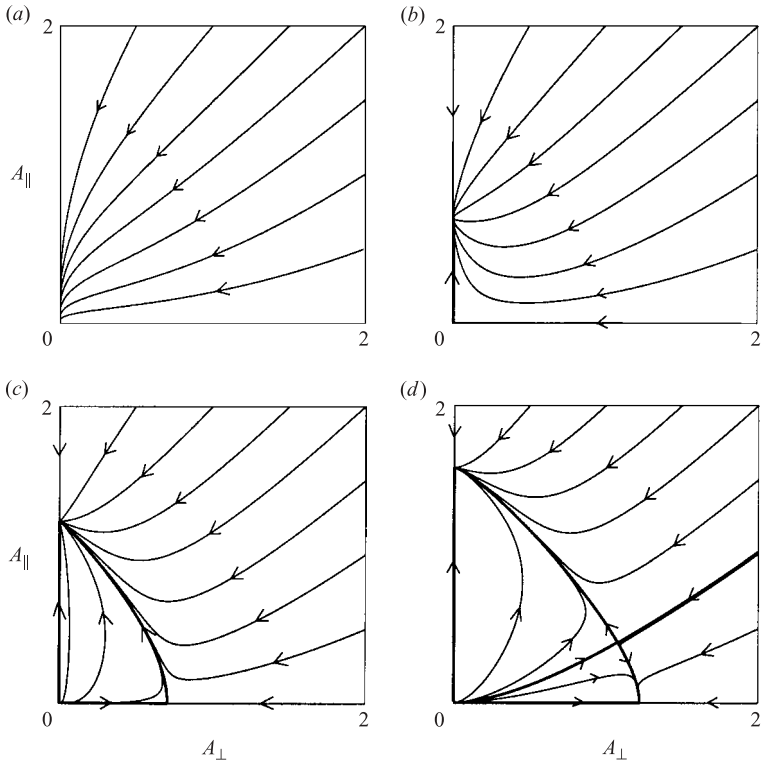

FIGURE 1. Phase-space trajectories of (1.1) for different values of r. (*a*) $r \leqslant 0$, the origin is the only sink. (*b*) $0 < r \leqslant \rho^2$, the origin is a saddle point and the point $A_\perp = 0$, $A_\parallel = r^{1/2}$ corresponding to LRs becomes a sink. (*c*) $\rho^2 < r \leqslant \rho^2(1+\beta^{-2})$, the origin is a source, the 'pure LR point' remains a sink and a saddle point emerges on the TR-axis. (*d*) $r > \rho^2(1+\beta^{-2})$, the saddle point on the TR-axis becomes a sink while a new saddle point, corresponding to a combination of TRs and LRs, emerges.

where $A_\perp$ and $A_\parallel$ are the amplitudes of the transverse and longitudinal rolls, respectively, while r and ρ are, up to real multiplicative constants, equal to $\epsilon^{-2}(\mathscr{R} - \mathscr{R}_c^{(\pi/2)})$ and $\epsilon^{-1}R$, respectively, with ϵ being a small expansion parameter. The real coefficient β is directly related to the interaction coefficient appearing in the RB problem (see Schlüter *et al.* 1965, for a quantitative evaluation) since the mean shear does not influence the nonlinear interactions at this order (note that β depends on the Prandtl number P). The main features of system (1.1) are shown in figure 1. For $r \leqslant 0$, $A_\perp = A_\parallel = 0$ is the stable solution. As r becomes positive, this solution becomes unstable and pure LRs emerge as a stable solution. TRs appear when $r > \rho^2$, but are unstable as long as $r < \rho^2(1+\beta^{-2})$. Finally, for $r \geqslant \rho^2(1+\beta^{-2})$, both LRs and TRs are stable with the final state strongly dependent on the initial condition. This state always consists of either LRs or TRs since a combined pattern with $A_\perp \neq 0$ and $A_\parallel \neq 0$ is unstable as in the case of the pure RB problem. Hence, nonlinear mechanisms increase the difference between the (linear) critical Rayleigh numbers for LRs and TRs, but nevertheless allow stable TR convection for sufficiently large values of $\mathscr{R}$. The preceding analysis remains valid for an arbitrary orientation φ of the roll with amplitude $A^{(\varphi)}$, provided ρ is replaced by $\rho\cos\varphi$ and the appropriate value of β is used.

The dependence of the final orientation of the roll pattern on the initial condition in the spatially homogeneous problem modelled by amplitude equations (1.1) may be roughly considered to be the temporal equivalent of the dependence of the final pattern on spatial constraints and inhomogeneities in a real laboratory experiment. The presence of lateral walls, as well as system in and outlet and spatial imperfections of the temperature profile on the upper and lower plates, for instance, are known to influence the pattern selection strongly. As in the RB case, such effects may be modelled by allowing slow spatial variations of the amplitude (and possibly of one or more parameters) in the multiple scale analysis used to derive envelope equations. Such an analysis has been performed by Walton (1985) for an RBP system in which a streamwise linear variation of the Rayleigh number is allowed. Walton's rigorous derivation of envelope equations highlights the main difficulties inherent in this approach which arise from the difference of the relevant scalings for different roll orientations. This is partly related to the convective nature of the RBP instability at marginality and the possible, orientation-dependent transition to absolute instability for supercritical Rayleigh numbers (Müller *et al.* 1992; Carrière & Monkewitz 1999). It is clear that a careful analysis of the convective–absolute nature of the instability patterns is required since, as originally outlined by Müller *et al.* (1992), it may play an important role in the competition between LRs and TRs. In the following, we extend the analysis of Walton (1985) by including slow variations of the amplitude in the transverse direction and more general variations of the Rayleigh number. According to our previous work (see Carrière & Monkewitz 1999), transition from convective to absolute instability only involves TRs. In contrast to this previous study, in which the stability problem was treated numerically, we are seeking here analytical solutions. In § 2, we derive envelope equation describing LRs for $O(1)$ Reynolds numbers and examine their stability properties. In § 3, analytical solutions are developed in the limit of small Reynolds numbers which allow an explicit determination of the Green function and hence are particularly useful for understanding the different behaviour of LRs and TRs. They also provide the starting point for a global mode analysis with two directions of wave propagation, presented in Part 2 (Martinand, Carrière & Monkewitz 2004). A general discussion of the results is proposed in § 4.

2. Finite $O(1)$ Reynolds number

The fluid layer, of depth h in the vertical z-direction, is assumed to be of infinite extent in the horizontal x- and y-directions and subjected to a pressure gradient in the x-direction so that a mean Poiseuille flow is established with non-dimensional velocity and pressure fields

$$\boldsymbol{U}_p = \tilde{U}_p(z)\,\boldsymbol{e}_x = (1-4z^2)\,\boldsymbol{e}_x, \tag{2.1a}$$

$$\Pi_p = -\frac{8}{R}x + \text{const.} \tag{2.1b}$$

In (2.1), the Reynolds number R is defined as

$$R = \frac{U_m h}{\nu}, \tag{2.2}$$

where U_m is the maximum of the Poiseuille velocity profile and ν is the kinematic viscosity of the fluid. Without loss of generality, the temperature of the upper wall is assumed to be at a constant value T_{*r} relative to which the temperature in the fluid is defined (here and in the following, $*$ denotes a dimensional quantity). Temperature

differences are scaled with respect to the quantity $\nu K/(g\alpha h^3)$ with g the acceleration due to gravity, α the thermal expansion coefficient and K the thermal diffusivity of the fluid. We assume that the (dimensional) lower wall temperature T_*^+ departs only slightly from the critical temperature for linear instability in the absence of throughflow. Introducing the critical Rayleigh number $\mathscr{R}_c^{(\pi/2)}$ for LRs (and the RB problem) and a small parameter ϵ, we can write

$$T_*^+ = T_{*r} + \frac{\nu\kappa}{g\alpha h^3}\left(\mathscr{R}_c^{(\pi/2)} + \epsilon^2\mathscr{R}_2\right), \tag{2.3}$$

where the small departure from criticality $\varepsilon^2\mathscr{R}_2$ can depend slowly on the x- and y-coordinates. For an $O(1)$ Reynolds number, as considered in this section, the appropriate scaling for the slow spatial coordinates is

$$x_1 = \epsilon x, \tag{2.4a}$$

$$y_1 = \epsilon y. \tag{2.4b}$$

In addition, the following successively slower time scales are introduced:

$$t_1 = \epsilon t, \quad t_2 = \epsilon^2 t. \tag{2.5}$$

To facilitate the distinction between different scalings, we denote the original $O(1)$ spatial and time coordinates x, y and t by x_0, y_0 and t_0.

As usual, the non-dimensional velocity $\boldsymbol{U}$, pressure Π and temperature T fields are expanded as

$$\boldsymbol{U} = \boldsymbol{U}_p + \epsilon\boldsymbol{u}_1 + \epsilon^2\boldsymbol{u}_2 + \epsilon^3\boldsymbol{u}_3 + \text{h.o.t.}, \tag{2.6a}$$

$$\Pi = \Pi_p + \Pi_0 + \epsilon p_1 + \epsilon^2 p_2 + \epsilon^3 p_3 + \text{h.o.t.}, \tag{2.6b}$$

$$T = T_0 + \epsilon\theta_1 + \epsilon^2\theta_2 + \epsilon^3\theta_3 + \text{h.o.t.}, \tag{2.6c}$$

with

$$T_0 = \mathscr{R}_c^{(\pi/2)}\left(\tfrac{1}{2} - z\right), \quad \Pi_0 = \frac{\mathscr{R}_c^{(\pi/2)}}{2} z(1-z) + \text{const.} \tag{2.7}$$

Details of the derivation and the solution of the successive problems are given in Appendix A. According to the linear stability analysis, for an $O(1)$ Reynolds number, only LRs are unstable since the Rayleigh number is $\mathscr{R}_c^{(\pi/2)}$ at leading order. The solution $\boldsymbol{v}_1 = (p_1, \boldsymbol{u}_1, \theta_1)^{\mathrm{T}}$ may thus be written

$$\boldsymbol{v}_1 = A\exp(\mathrm{i}k_c y_0)\boldsymbol{V}_1(z) + \text{c.c.}, \tag{2.8}$$

with $\boldsymbol{V}_1$ given in Appendix A and c.c. denoting the complex conjugate. The amplitude A in (2.8) is an implicit function of the slow variables $A = A(x_1, y_1, t_1, t_2)$.

As detailed in Appendix A, a non-trivial equation is obtained from the solvability condition of the problem at $O(\epsilon^2)$ owing to the convective nature of the instability:

$$\partial_{t_1} A + R\,c\,\partial_{x_1} A = 0. \tag{2.9}$$

As recognized early on by Stewartson & Stuart (1971), the solution of (2.9) is a wave propagating at group velocity $R\,c$:

$$A = A(\chi_1, y_1, t_2) \text{ with } \chi_1 = x_1 - R\,c\,t_1. \tag{2.10}$$

Our numerical evaluation of c gives:

$$c = P\,\frac{0.4718 + 1.375P}{0.8012 + 1.566P}, \tag{2.11}$$

in agreement with the results of Walton (1985) so that Rc is strictly positive except in the limits $R \to 0$ or $P \to 0$. Thus, the instability remains convective and, as a consequence, the next order approximation describes the evolution of the wave in the frame of reference moving at the group velocity. It is noteworthy that this envelope formalism cannot capture a transition from convective to absolute instability, even if it existed, for an $O(1)$ Reynolds number since it would involve at least an $O(1)$ difference between the critical Rayleigh number for convective instability and the Rayleigh number for convective–absolute transition (the ansatz (2.3) only allows an $O(\epsilon^2)$ difference). This is in full agreement with our previous analysis of this problem where no convective–absolute transition was detected for LRs for $R = O(1)$ and physically relevant values of the Rayleigh number (Carrière & Monkewitz 1999).

At the next order, the following envelope equation for the complex amplitude A is obtained

$$\tau\,\partial_{t_2} A = \mu\,\mathscr{R}_2\,A + \alpha R^2\,\partial^2_{\chi_1} A + \mathrm{i}\eta R\,\partial_{\chi_1}\partial_{y_1} A + \xi\,\partial^2_{y_1} A - \lambda\,A^2\overline{A}. \tag{2.12}$$

The numerical values for the various constants appearing in equation (2.12) are (cf. Appendix A):

$$\tau = P^{-1}(0.8012 + 1.566P), \tag{2.13a}$$

$$\mu = 0.018, \tag{2.13b}$$

$$\alpha = 10^{-2}(\tau P)^{-2}(0.004359 + 0.004804P + 0.4436P^2 + 0.0735P^3 + 0.0849P^4), \tag{2.13c}$$

$$\eta = (\tau P)^{-1}(0.05523 + 0.01103P + 0.04263P^2), \tag{2.13d}$$

$$\xi = 4.555. \tag{2.13e}$$

$$\lambda = 0.7753 - \frac{0.005229}{P} + \frac{0.009228}{P^2}. \tag{2.13f}$$

The Landau constant λ is taken from Schlüter *et al.* (1965). All these coefficients are strictly positive for any non-zero value of the Prandtl number. By the simple change of variables:

$$t_2 \to \tau^{-1}t_2,\ A \to \lambda^{1/2}A,\ \chi_1 \to R^{-1}\alpha^{-1/2}\chi_1,\ y_1 \to \xi^{-1/2}y_1,\ \eta \to (\alpha\xi)^{-1/2}\eta, \tag{2.14}$$

and by setting

$$r = \mu\mathscr{R}_2, \tag{2.15}$$

(2.12) is reduced to the generic form:

$$\partial_{t_2} A = r\,A + \partial^2_{\chi_1} A + \mathrm{i}\eta\,\partial_{\chi_1}\partial_{y_1} A + \partial^2_{y_1} A - A^2\overline{A}, \tag{2.16}$$

where the influence of the Reynolds number is now hidden in the redefinition of χ_1. Equation (2.12) is relevant for $O(1)$ values of R sufficiently below the critical Reynolds number for Tollmien–Schlichting type instabilities where, according to Fujimura & Kelly (1995), an additional equation would have to be introduced.

Equation (2.16) has the classical phase winding solutions

$$A_0 = (r - a^2 - b^2)^{1/2}\exp(\mathrm{i}\,(a\chi_1 + by_1 - \eta abt_2 + \phi_0))\,, \tag{2.17}$$

with wavenumbers a and b in the directions of χ_1 and y_1 and ϕ_0 an arbitrary constant phase, provided $r > a^2 + b^2$. The linear stability of such a solution is investigated by adding a small perturbation B to the solution A_0:

$$A = A_0 + B\,(\chi_1, y_1, t_2)\exp(\mathrm{i}\,(a\chi_1 + by_1 - \eta abt_2 + \phi_0))\,. \tag{2.18}$$

The equation for B, linearized around A_0, is obtained as

$$\partial_{t_2} B = -(r - a^2 - b^2)(B + \overline{B}) + (-\eta b + 2\mathrm{i}a)\ \partial_{\chi_1} B + (-\eta a + 2\mathrm{i}b)\ \partial_{y_1} B + \partial^2_{\chi_1} B + \mathrm{i}\gamma\ \partial^2_{\chi_1}\partial_{y_1} B + \partial^2_{y_1} B. \tag{2.19}$$

With the ansatz

$$B = B_1 \exp(\mathrm{i}(a'\chi_1 + b' y_1 - \omega' t_2)) + \overline{B}_2 \exp(-\mathrm{i}(a'\chi_1 + b' y_1 - \overline{\omega'} t_2)), \tag{2.20}$$

where B_1 and B_2 are two complex constants, we obtain a dispersion relation which is quadratic in ω' and yields the eigenvalues

$$\omega'_{\pm} = \sigma q k' - \mathrm{i}(r' + q^2) \pm \mathrm{i}(r'^2 + q^2(2k'\zeta + \mathrm{i}\eta' q)^2)^{-1/2}. \tag{2.21}$$

In (2.21), the following abbreviations have been introduced for convenience:

$$\left.\begin{aligned} &k'^2 = a^2 + b^2,\ r' = r - k'^2,\ q^2 = a'^2 + b'^2,\ \eta' = \eta q^{-2} a' b', \\ &\zeta = (k'q)^{-1}(aa' + bb'),\ \sigma = \eta(k'q)^{-1}(ab' + ba'). \end{aligned}\right\} \tag{2.22}$$

The root ω'_- of (2.21) has an imaginary part which remains negative since A_0 exists only for $r' > 0$. For the phase winding solution to be stable, $\mathrm{Im}(\omega'_+)$ has to be negative as well, which is the case if the real part of the square root in (2.21) is smaller than $r' - q^2$. After some algebra, this condition may be expressed as:

$$q^2[(1 + \eta'^2)q^6 + 2(r' + (r' - 2k'^2\zeta^2)(1 + \eta'^2))q^4 + (r'^2(1 + \eta'^2) + 4r'(r' - 2k'^2\zeta^2))q^2 + 2r'^2(r' - 2k'^2\zeta^2)] > 0. \tag{2.23}$$

Clearly, the coefficients of the polynomial in q^2 are positive as long as $r' > 2k'^2\zeta^2$. On the other hand, when $r' < 2k'^2\zeta^2$ the last coefficient is negative, implying negative values of the polynomial in some regions around $q = 0$. In terms of the original r, phase winding solutions are thus stable if $r > (1 + 2\zeta^2)k'^2$. Since ζ is the cosine of the angle between the wavevector of the phase winding solution and of the perturbation, the most restrictive condition is obtained for $\zeta = 1$, for which the Eckhaus criterion is recovered:

$$k'^2 < \tfrac{1}{3} r. \tag{2.24}$$

This simply means that the most dangerous instability of a given phase winding solution of (2.16) has the same wavevector orientation as the solution itself.

Provided (2.24) is satisfied, the envelope equation (2.16) thus predicts the existence of stable longitudinal convection rolls, which may be slowly modulated in the horizontal direction, above the RB threshold of $\mathscr{R}_c^{(\pi/2)} \approx 1707$. This result fully agrees with the known experimental observations at moderately large Reynolds numbers. Considering that equation (2.16) is only valid in a moving frame of reference, the temporal evolution in (2.16) mimics the spatial evolution (amplification) of finite-amplitude inlet perturbations into LRs. This naturally leads to the question of what happens when other kinds of perturbations, more specifically TRs, are also amplified. This question implies that the critical Rayleigh number is of the same order for all wavevector orientation, meaning that, in the present formalism, the analysis must be restricted to small Reynolds numbers. This is the subject of the following section.

3. Envelope equations for infinitesimal R

3.1. *Envelope equations for* $R = O(\epsilon^{3/2})$

The multiple scale analysis must be modified when considering values of R of the order of some power of the small parameter ϵ. As already remarked by Walton (1985), two different scalings for R, corresponding to different behaviour of the system, can be chosen. The very low Reynolds-number limit may be investigated by setting

$$R = \epsilon^{3/2} R_{3/2}. \tag{3.1}$$

With this scaling, the $O(\epsilon)$ problem reduces to the Rayleigh–Bénard problem in the absence of mean through-flow. Hence, no mode orientation is selected at the linear stage and the analysis may be performed for a roll of arbitrary orientation φ, recalling that φ has been defined as the angle between the horizontal wavevector and the streamwise direction. It is then more convenient to use x' and y' axes normal and tangential to the roll axis, respectively. The relevant scalings for these coordinates are

$$x'_1 = \epsilon x', \quad y'_{1/2} = \epsilon^{1/2} y', \tag{3.2}$$

while the appropriate time scales are

$$t_{3/2} = \epsilon^{3/2} t, \quad t_2 = \epsilon^2 t. \tag{3.3}$$

At first order, the roll solution $\boldsymbol{v}_{1,\varphi} = (p_{1,\varphi}, \boldsymbol{u}_{1,\varphi}, \theta_{1,\varphi})^{\mathrm{T}}$ is given by

$$\boldsymbol{v}_{1,\varphi} = A_\varphi \exp\left(\mathrm{i}k_c \left(x'_0 - R_{3/2}\, c\, \cos\varphi\, t_{3/2}\right)\right) \boldsymbol{V}_{1,\varphi}(z) + \text{c.c.}, \tag{3.4}$$

with c given by (2.11) and $A_\varphi = A_\varphi(x'_1, y'_{1/2}, t_2)$. Note that, as expected, roll modes (except LRs) are travelling waves in the presence of a mean shear, with phase speed proportional to R and to $\cos\varphi$ (see Müller 1990). The analysis detailed in Appendix B.1 yields the envelope equation for A_φ:

$$\tau\, \partial_{t_2} A_\varphi = \mu \mathscr{R}_2 A_\varphi + \tau\, R_{3,2}\, c\, \sin\varphi\, \partial_{y'_{1/2}} A_\varphi + \xi \left(\partial_{x'_1} + (2\mathrm{i}k_c)^{-1} \partial^2_{y'_{1/2}}\right)^2 A_\varphi - \lambda A_\varphi^2 \overline{A}_\varphi, \tag{3.5}$$

which is just the Newell–Whitehead–Segel equation (see Newell & Whitehead 1969; Segel 1969) obtained for zero through-flow with an additional convection term proportional to the Reynolds number times the sine of the angle between the wavevector and the streamwise direction. The definition of the various coefficients appearing in (3.5) is the same as in the previous section. Thus, (3.5) may be simplified by the following change of variables:

$$t_2 \to \tau^{-1} t_2, \;\; A_\varphi \to \lambda^{1/2} A_\varphi, \;\; x'_1 \to \xi^{-1/2} x'_1, \;\; y'_{1/2} \to \left(2k_c\, \xi^{-1/2}\right)^{1/2} y'_{1/2}. \tag{3.6}$$

Setting furthermore

$$\tilde{c} = \tau c \left(\tfrac{1}{2}\alpha k_c\, \xi^{1/2}\right)^{-1/2}, \quad \rho = \alpha^{1/2} k_c R_{3/2}, \tag{3.7}$$

where the coefficient α has been introduced for coherence with the future equation (3.17), equation (3.5) becomes

$$\partial_{t_2} A_\varphi = r A_\varphi + \rho \tilde{c}\, \sin\varphi\, \partial_{y'_{1/2}} A_\varphi + \left(\partial_{x'_1} - \mathrm{i}\partial^2_{y'_{1/2}}\right)^2 A_\varphi - A_\varphi^2 \overline{A}_\varphi, \tag{3.8}$$

with r as defined by (2.15).

Since, in the local stability analysis of (3.8), the additional convective term only contributes to the oscillatory part of the instability mode, the critical values for local instability are the same as for the Newell–Whitehead–Segel equation. For the analysis

of the nature of the instability, convective or absolute, it is convenient to go back to the Green function rather than trying to directly apply the Briggs (1964) criterion (see Brevdo 1991; Carrière & Monkewitz 1999, for its application in the case of two wave propagation directions). After successive Fourier transforms in the $y'_{1/2}$ (wavenumber b), x'_1 (wavenumber a) and t_2 (frequency $-\omega$) directions, the response of the linear part of (3.8) to an impulse $\delta(x'_1)\delta(y'_{1/2})\delta(t_2)$ is easily found to be

$$\hat{\hat{\hat{G}}}(a, b, \omega) = (-\mathrm{i}\omega - r - \mathrm{i}b\rho\tilde{c}\sin\varphi + (a + b^2)^2)^{-1}. \tag{3.9}$$

The inverse Fourier transform in time is performed, as usual, along a contour in the complex ω-plane which is a straight line parallel to the real axis located above all the singularities (i.e. such that $\mathrm{Im}(\omega) > r$) to satisfy the causality condition. Closing the contour in the lower ω-plane and evaluating residues, we obtain for $t_2 > 0$

$$\hat{\hat{\hat{G}}}(a, b, t_2) = -\exp((r - \mathrm{i}b\rho\tilde{c}\sin\varphi + (a + b^2)^2)t_2). \tag{3.10}$$

Since the argument of the exponential is a quadratic form in a, the inverse Fourier transform of $\hat{\hat{\hat{G}}}$ in the a-direction can be performed analytically (see Champeney 1973, p. 22):

$$\hat{G}(x'_1, b, t_2) = -\frac{1}{2(\pi t_2)^{1/2}} \exp\left[\left(r - \left(\frac{1}{2}\frac{x'_1}{t_2}\right)^2 + \mathrm{i}b\rho\tilde{c}\sin\varphi - \mathrm{i}b^2\frac{x'_1}{t_2}\right)t_2\right]. \tag{3.11}$$

Finally, the Green function in physical space is obtained by inverting the Fourier transform in the b-direction (Champeney 1973, p. 38) with the result

$$G(x'_1, y'_{1/2}, t_2) = -\frac{\exp(-\mathrm{i}\pi/4)}{4\pi t_2}\left(\frac{x'_1}{t_2}\right)^{-1/2} \exp\left[\left(r - \left(\frac{1}{2}\frac{x'_1}{t_2}\right)^2\right)t_2\right] \times \exp\left[\mathrm{i}\left(4\frac{x'_1}{t_2}\right)^{-1}\left(\rho\tilde{c}\sin\varphi + \frac{y'_{1/2}}{t_2}\right)^2 t_2\right]. \tag{3.12}$$

The convective–absolute nature of the instability is determined by the limiting behaviour of $G(x'_1, y'_{1/2}, t_2)$ as $t_2 \to \infty$ along the particular ray $x'_1/t_2 = y'_{1/2}/t_2 = 0$. Considering the clearly singular limit $x'_1/t_2 \to 0$ in (3.12) yields

$$\lim_{x'_1/t_2 \to 0} G(x'_1, y'_{1/2}, t_2) = -\frac{1}{2\pi^{1/2}t_2}\exp(rt_2)\,\delta\left(t_2^{1/2}\left(\rho\tilde{c}\sin\varphi + \frac{y'_{1/2}}{t_2}\right)\right). \tag{3.13}$$

Hence, along the ray $x'_1/t_2 = 0$, G is a Dirac delta function moving at velocity $-\rho\tilde{c}\sin\varphi$ along the $y'_{1/2}$-direction. Thus, the impulse response is 0 along the ray $x'_1/t_2 = y'_{1/2}/t_2 = 0$ for all modes except TRs, since in this case $\sin\varphi = 0$ and the delta function remains stationary while experiencing unbounded growth in t_2. The different possibilities are sketched in figure 2.

Therefore, the key result obtained from the envelope equation (3.8) is that, in the presence of even a weak mean Poiseuille through-flow, all instability modes except transverse rolls are convectively unstable, in agreement with our earlier findings (Carrière & Monkewitz 1999). Further investigations based on (3.8) therefore do not appear to be of interest and we seek further insight into the problem by increasing R to $O(\epsilon)$ as detailed in the next subsection.

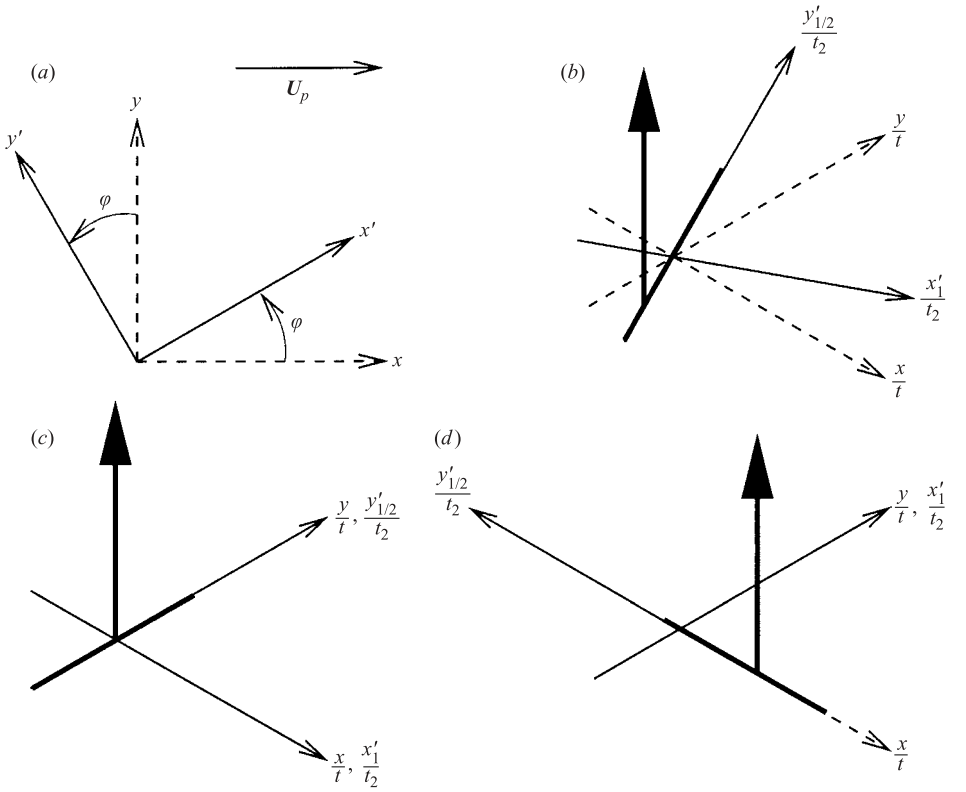

FIGURE 2. Sketch of the impulse response for $R = O(\epsilon^{3/2})$. Only the response along the ray $x'_1/t_2 = 0$ is represented, where the Dirac delta function is symbolized by a vertical arrow. (*a*) Definition of the x'- and y'-directions. (*b*) Impulse response for arbitrary φ. (*c*) $\varphi = 0$ (TRs). (*d*) $\varphi = \pi/2$ (LRs).

3.2. *Envelope equations for* $R = O(\epsilon)$

The Reynolds number is increased by modifying (3.1) to

$$R = \epsilon R_1, \tag{3.14}$$

which requires the introduction of the additional time scale $t_1 = \epsilon t$ in order to allow rolls to travel at speeds of $O(R)$. The oscillatory behaviour of rolls is thus promoted to the time scale t_1:

$$\boldsymbol{v}'_{1,\varphi} = A_\varphi \exp(\mathrm{i}k_c(x'_0 - R_1\, c\, \cos\varphi\, t_1))\boldsymbol{V}_{1,\varphi}(z) + \text{c.c.} \tag{3.15}$$

As detailed in Appendix B.2, the solvability condition at $O(\epsilon^{5/2})$ implies that (cf. the previous subsection for the justification of the frame of reference $\upsilon'_{1/2}$)

$$A_\varphi = A_\varphi(x'_1, \upsilon'_{1/2}, t_2) \quad \text{with } \upsilon'_{1/2} = y'_{1/2} + R_1 c \sin\varphi t_{3/2}. \tag{3.16}$$

This leads at the next order in ϵ to the envelope equation

$$\begin{aligned}\tau\,\partial_{t_2} A_\varphi = {} & \left(\mu\mathscr{R}_2 - \alpha R_1^2 k_c^2 \cos^2\varphi\right) A_\varphi - R_1(\tau\, c + k_c\eta)\cos\varphi\, \partial_{x'_1} A_\varphi \\ & + \tfrac{1}{2} i\, R_1 \eta\, \cos\varphi\, \partial^2_{\upsilon'_{1/2}} A_\varphi + \xi\left(\partial_{x'_1} + (2\mathrm{i}k_c)^{-1}\partial^2_{\upsilon'_{1/2}}\right)^2 A_\varphi - \lambda A_\varphi^2 \overline{A}_\varphi,\end{aligned} \tag{3.17}$$

which describes the spatio-temporal behaviour of A_φ in a frame of reference moving at the group velocity $-R_1 c \sin\varphi$ along the $y'_{1/2}$-direction. With the change of variables (3.6), the redefinitions

$$c \to \tau c\, k_c^{-1}(\alpha\xi)^{-1/2}, \quad \eta \to (\alpha\xi)^{-1/2}\eta, \quad \rho = \alpha^{1/2} k_c R_1, \tag{3.18}$$

and r as defined by (2.15), (3.17) may be rewritten as

$$\partial_{t_2} A_\varphi = (r - \rho^2\cos^2\varphi)A_\varphi - \rho(c+\eta)\cos\varphi\, \partial_{x'_1} A_\varphi + \mathrm{i}\rho\eta\, \cos\varphi\, \partial^2_{\upsilon'_{1/2}} A_\varphi + \left(\partial_{x'_1} - \mathrm{i}\partial^2_{\upsilon'_{1/2}}\right)^2 A_\varphi - A_\varphi^2 \overline{A}_\varphi. \tag{3.19}$$

Envelope equation (3.19) is an extension of the amplitude equation of Richter (1973) and consequently has the same critical values of the control parameter for local instability, i.e.:

$$r_{\varphi,c} = \rho^2\, \cos^2\varphi. \tag{3.20}$$

In other terms, the critical Rayleigh number depends on both the square of the Reynolds number and the square of the cosine of the wavevector angle. All instability modes, including TRs, are now of convective type at marginality. According to § 3.1, no transition to absolute instability occurs when $\varphi \neq 0$. For TRs, on the other hand, equation (3.19) predicts such a transition. Indeed, proceeding as in § 3.1, the following expression for the Green function associated with (3.19) is obtained in the particular case $\varphi = 0$:

$$G(x'_1, y'_{1/2}, t_2) = -\frac{\exp(-\mathrm{i}\pi/4)}{4\pi t_2}\left(\frac{x'_1}{t_2} - \rho c\right)^{-1/2} \exp\left[\left\{r - \rho^2\left(1 + \frac{(c+\eta)^2}{4}\right) - \frac{1}{2}\frac{x'_1}{t_2}\left(\frac{x'_1}{t_2} - \rho\frac{c+\eta}{2}\right)\right\} t_2\right] \exp\left[\mathrm{i}\left(4\left(\frac{x'_1}{t_2} - \rho c\right)\right)^{-1}\left(\frac{y'_{1/2}}{t_2}\right)^2 t_2\right]. \tag{3.21}$$

At sufficiently low positive values of $r - \rho^2$, the instability is convective since the growing part of the wave packet described by (3.21) is entirely contained between the two rays given by $x'_1/t_2 = \rho(c+\eta) \pm 2(r-\rho^2)^{1/2}$. Increasing r while holding ρ fixed thus leads to a transition to absolute instability when $r > r_\mathrm{a}$ with

$$r_\mathrm{a} - \rho^2 = \rho^2\frac{(c+\eta)^2}{4}. \tag{3.22}$$

4. Discussion

Including both streamwise and transverse wave propagation directions, the analysis of § 3 has revealed the subtle behaviour of the linear impulse response of the RBP system at low Reynolds numbers. The group velocity here being proportional to the Reynolds number, it has allowed the complete determination of the convective or absolute nature of any instability pattern. However, the reader is reminded that the analysis is restricted to RB-like patterns slowly modulated by the through-flow. Therefore, because of the absolute nature of the instability in the RB problem, the absolute wavenumber is real at leading order, with a complex first-order correction. Returning to figure 2, the Green function which, in the $y'_{1/2}$-direction (i.e. the roll-axis direction), remains a Dirac delta function located at a negative value of $y'_{1/2}/t_2$, prevents any upstream propagation of the impulse response and thus any possibility of

a convective/absolute transition, except for TRs. Owing to the singular nature of the Green function, the determination of saddle-points of the dispersion relation becomes singular as the $y'_{1/2}/t_2$-axis is approached, as only one saddle-point, corresponding to the location of the Dirac delta function, subsists along this axis. The analytical determination of the Green function, made possible in the simplified framework of envelope formalism, clarifies our previous analysis of the general case (Carrière & Monkewitz 1999), which used steepest descent techniques to evaluate the asymptotic behaviour of the Green function and where the disappearance of the saddle-point for $x/t \to 0$ left some uncertainty about the effective behaviour of the Green function. For the particular case of TRs, the present results are qualitatively in agreement with the results of Müller *et al.* (1992), even though their envelope equation is different from ours.

More generally, the study highlights the complexity of the competition between LRs and TRs in the RBP system. On the one hand, for any non-zero value of the Reynolds number, the smallest critical Rayleigh number for convective instability always pertains to LRs. Furthermore, LRs are found to be a possible stable finite-amplitude pattern. Owing to their convective nature, LRs are, however, expected in a real experiment of finite length to appear as a result of spatial streamwise amplification of external noise at the inlet. The critical Rayleigh number for convective instability of TRs, on the other hand, is increasing with the square of the Reynolds number. Nevertheless, as the TR instability becomes absolute for sufficiently high values of the Rayleigh number, TR patterns can invade the entire RBP cell, including the vicinity of the inlet, irrespective of the level of external noise in the experiment. This is believed to explain the experimentally observed transition from LR to TR pattern in RBP convection when the Rayleigh number is increased at a fixed low value of the Reynolds number (see Luijkx *et al.* 1981; Ouazzani *et al.* 1989, 1990, 1995; Schröder & Bühler 1995; Chang *et al.* 1997; Yu *et al.* 1997).

A more complete exploration of such a transition in the somewhat unrealistic spatially homogeneous case would require interactions between TRs and LRs. Owing to the disparity of the relevant spatial scalings, it is at this point not clear how to include such interactions in the envelope equation formalism. Nevertheless, we can compare the critical Rayleigh numbers for stability of finite-amplitude TRs with respect to LRs, as given in § 1, and for the transition to absolute instability. Since both the Rayleigh numbers are quadratic functions of the Reynolds number in the limit studied, we show the ratio $\mathscr{R}_2/R_1^2$ as a function of the Prandtl number P in figure 3. It first shows the rapid increase of the absolute Rayleigh number with P, in agreement with our previous results (Carrière & Monkewitz 1999). Secondly, the stability curve always stays below the convective–absolute transition which suggests that absolutely unstable finite-amplitude TRs, are stable with respect to LRs. It is noted, however, that this result is restricted to low Reynolds numbers. At larger R, there is no evidence that the last conclusion remains true. Indeed, in most experiments no TR patterns have been found at higher Reynolds number. Finally, rolls with arbitrary orientation $0 < \varphi < \pi/2$ do not play a major role in this scenario, since such rolls are at most convectively unstable like LRs, but have a smaller growth rate.

With the homogeneous case essentially clarified, the analysis has to be extended to include spatial inhomogeneities in order to model real experiments better. A first analysis of this kind has been carried out by Carrière & Monkewitz (2001) in the framework of the Navier–Stokes equations for TRs varying slowly in the streamwise direction (i.e. without transverse variation). Equation (3.19) now offers a simplified framework to extend the so-called global mode analysis to the case of base states

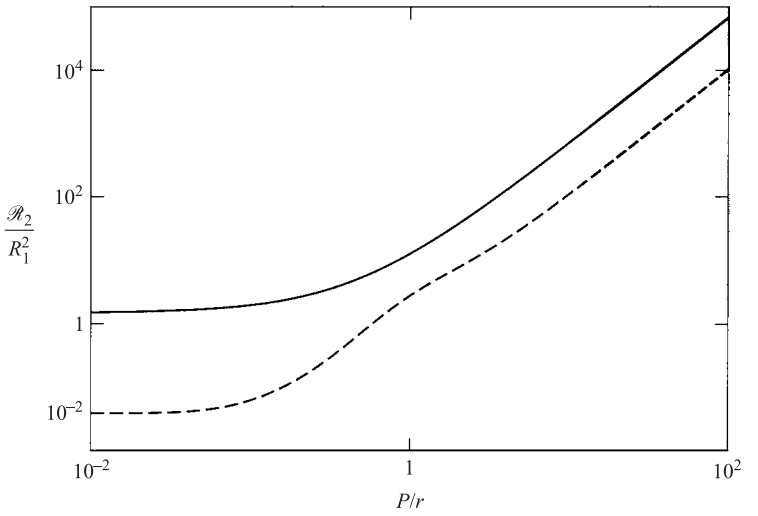

FIGURE 3. Ratio between the distance to the critical Rayleigh number $\mathscr{R}_2$ for TRs (dotted line, finite-amplitude stability curve; solid line, convective–absolute transition) and the square of the Reynolds number R_1 as a function of the Prandtl number P.

which are varying slowly in both horizontal directions and give rise to roll patterns with two wave-propagation directions. This program is the subject of Part 2.

The financial support of the ERCOFTAC Leonhard Euler Center, the Direction des Relations Internationales of the CNRS (Ph. C.) and the DERTT of the Région Rhône-Alpes (D. M.) is gratefully acknowledged.

Appendix A. Successive solutions of the multiple scale analysis at finite R

In the following, the notation $\mathscr{D} = \mathrm{d}/\mathrm{d}z$ is used throughout.

A.1. *Solution of the first-order problem*

At first order, the set of linear homogeneous equations for $\boldsymbol{v}_1 = [p_1, \boldsymbol{u}_1, \theta_1]^{\mathrm{T}}$ and its associated eigenvalue $-\mathrm{i}\omega$ is given by

$$\mathscr{L}_0 \boldsymbol{v}_1 = 0, \tag{A 1}$$

where $\mathscr{L}_0 \boldsymbol{v}_1$ is defined by

$$\begin{aligned}\mathscr{L}_0 \boldsymbol{v}_1 = \big[&-\nabla_0 \cdot \boldsymbol{u}_1, -\mathrm{i}\omega P^{-1}\boldsymbol{u}_1 + R(U_p\, \partial_{x_0}\boldsymbol{u}_1 + \mathscr{D}U_p(\boldsymbol{u}_1 \cdot \boldsymbol{e}_z)\boldsymbol{e}_x) + \nabla_0 p_1 - \theta_1 \boldsymbol{e}_z \\ &- \nabla_0^2 \boldsymbol{u}_1, -\mathrm{i}\omega\theta_1 + RPU_p \partial_{x_0}\theta_1 - \mathscr{R}_c^{(\pi/2)}\boldsymbol{u}_1 \cdot \boldsymbol{e}_z - \nabla_0^2\theta_1\big]^{\mathrm{T}}\end{aligned} \tag{A 2}$$

and ∇_0 stands for

$$\nabla_0 = \left(\partial_{x_0},\ \partial_{y_0},\ \partial_z\right)^{\mathrm{T}}. \tag{A 3}$$

The boundary conditions for $\boldsymbol{v}_1$ in (A 1) are

$$\boldsymbol{u}_1(z = \pm 1/2) = \theta_1(z = \pm 1/2) = 0. \tag{A 4}$$

For LRs as in (2.8), (A 1) reduces to the usual RB problem, except for a non-zero component of the velocity in the x-direction. The z-dependence of LR modes is thus

of the form

$$\boldsymbol{V}_1 = \left[P_1,\ Rk_c^{-2}U_1,\ \mathrm{i}k_c^{-1}V_1,\ W_1,\ \Theta_1\right]^{\mathrm{T}}, \tag{A 5}$$

with W_1 as originally determined by Pellew & Southwell (1940):

$$W_1 = \sum_{n=1}^{n=3} C_n \cosh q_n z. \tag{A 6}$$

In the present paper, we use the following numerically determined values for the constants:

$$\mathscr{R}_c^{(\pi/2)} = 1707.76177,\ k_c = 3.116323555, \tag{A 7a}$$

$$C_1 = 1.0,\ C_2 = -0.0307641793 + \mathrm{i}\,0.0519556612,\ C_3 = \overline{C_2}, \tag{A 7b}$$

$$q_1 = \mathrm{i}\,3.973704179,\ q_2 = 5.194390868 - \mathrm{i}\,2.125870478,\ q_3 = \overline{q_2}. \tag{A 7c}$$

The functions V_1, P_1 and Θ_1 are then deduced from W_1 by the following relations:

$$V_1 = \mathscr{D}W_1, \tag{A 8a}$$

$$P_1 = \left(k_c^{-2}\mathscr{D}^2 - 1\right)V_1(z), \tag{A 8b}$$

$$\Theta_1 = k_c^2\left(k_c^{-2}\mathscr{D}^2 - 1\right)^2 W_1(z). \tag{A 8c}$$

The function U_1 satisfies the equation:

$$\left(k_c^{-2}\mathscr{D}^2 - 1\right)U_1 = W_1\,\mathscr{D}U_p. \tag{A 9}$$

The solution has the form:

$$U_1 = D_0 \sinh(k_c z) + \sum_{n=1}^{n=3} E_n z \cosh q_n z + F_n \sinh q_n z, \tag{A 10}$$

where E_n and F_n are given by

$$E_n = 8k_c^2 C_n\left(k_c^2 - q_n^2\right)^{-1}, \quad F_n = 16k_c^2 q_n C_n\left(k_c^2 - q_n^2\right)^{-2} \tag{A 11}$$

and the value of D_0 is determined by imposing $U_1(1/2) = 0$.

A.2. *Adjoint problem*

Proceeding to higher orders in the expansion requires the determination of the adjoint mode. In the present case, the appropriate scalar product is

$$\langle \boldsymbol{v}_\iota,\ \boldsymbol{v}_\jmath \rangle = \lim_{X,Y\to\infty} \frac{1}{4XY} \int_{-X}^{X}\int_{-Y}^{Y}\int_{-1/2}^{1/2} \boldsymbol{v}_\iota \cdot \overline{\boldsymbol{v}}_\jmath \,\mathrm{d}x\,\mathrm{d}y\,\mathrm{d}z. \tag{A 12}$$

With this definition, the adjoint operator of $\mathscr{L}_0$ in (A 1) is given by

$$\begin{aligned}\mathscr{L}_0^\star \boldsymbol{v}_1^\star = \big[&-\nabla_0 \cdot \boldsymbol{u}_1^\star,\ \mathrm{i}\overline{\omega}P^{-1}\boldsymbol{u}_1^\star - R\left(U_p\partial_{x_0}\boldsymbol{u}_1^\star - \mathscr{D}\boldsymbol{U}_p\,(\boldsymbol{u}_1^\star\cdot\boldsymbol{e}_x)\boldsymbol{e}_z\right) + \nabla p_1^\star - \mathscr{R}_c^{(\pi/2)}\theta_1^\star\boldsymbol{e}_z \\ &- \nabla_0^2\boldsymbol{u}_1^\star,\ \mathrm{i}\overline{\omega}\,\theta_1^\star - RPU_p\partial_{x_0}\theta_1^\star - \boldsymbol{u}_1^\star\cdot\boldsymbol{e}_z - \nabla_0^2\theta_1^\star\big]^{\mathrm{T}}.\end{aligned} \tag{A 13}$$

The eigenvalue $-\mathrm{i}\omega$ vanishes identically for longitudinal rolls at criticality and thus we easily finds the adjoint longitudinal roll mode

$$\boldsymbol{v}_1^\star = \exp(\mathrm{i}k_c y_0)\boldsymbol{V}_1^\star(z), \tag{A 14}$$

where $\boldsymbol{V}_1^\star$ is given by

$$\boldsymbol{V}_1^\star = \left[P_1,\ 0,\ \mathrm{i}k_c^{-1}V_1,\ W_1,\ \mathscr{R}_c^{(\pi/2)^{-1}}\Theta_1\right]^{\mathrm{T}}. \tag{A 15}$$

A.3. *Second-order solvability condition*

At $O(\epsilon^2)$, the non-homogeneous problem for $\boldsymbol{v}_2 = [p_2, \boldsymbol{u}_2, \theta_2]^{\mathrm{T}}$ is

$$\mathscr{L}_0 \boldsymbol{v}_2 = \mathscr{S}_2(\boldsymbol{v}_1), \tag{A 16}$$

where $\mathscr{S}_2(\boldsymbol{v}_1)$ reads:

$$\mathscr{S}_2(\boldsymbol{v}_1) = \big[\nabla_1 \cdot \boldsymbol{u}_1,\ -P^{-1}(\partial_{t_1}\boldsymbol{u}_1 + (\boldsymbol{u}_1 \cdot \nabla_0)\boldsymbol{u}_1) - RU_p\,\partial_{x_1}\boldsymbol{u}_1 - \nabla_1 p_1 + 2\,\partial_{y_1}\partial_{y_0}\boldsymbol{u}_1,$$
$$-\partial_{t_1}\theta_1 - \boldsymbol{u}_1 \cdot \nabla_0\theta_1 - RPU_p\,\partial_{x_1}\theta_1 + 2\,\partial_{y_1}\partial_{y_0}\theta_1\big]^{\mathrm{T}} \tag{A 17}$$

and ∇_1 stands for

$$\nabla_1 = (\partial_{x_1},\ \partial_{y_1},\ 0)^{\mathrm{T}}. \tag{A 18}$$

The boundary conditions for $\boldsymbol{v}_2$ in (A 16) are

$$\boldsymbol{u}_2(z = \pm 1/2) = \theta_2(z = 1/2) = 0, \quad \theta_2(z = -1/2) = \mathscr{R}_2. \tag{A 19}$$

Since LRs are stationary, the condition for the solvability of (A 16) reduces to

$$\langle \mathscr{S}_2(\boldsymbol{v}_1),\ \boldsymbol{v}_1^{\star}\rangle = 0, \tag{A 20}$$

which leads to

$$\partial_{t_1} A + \partial_{k_x}\omega|_c \partial_{x_1} A + \partial_{k_y}\omega|_c \partial_{y_1} A, \tag{A 21}$$

where we used the notation

$$\partial_{k_x}\omega|_c = \partial_{k_x}\omega|_{k_x=0,k_y=k_c},\ \partial_{k_y}\omega|_c = \partial_{k_y}\omega|_{k_x=0,k_y=k_c}. \tag{A 22}$$

Note that quadratic interaction does, as usual, not provide any resonant terms in (A 21). Since LRs are the most amplified modes, we have

$$\partial_{k_x}\omega_i|_c = \partial_{k_y}\omega_i|_c = 0, \tag{A 23}$$

and, since all modes with $k_x = 0$ are stationary, we also have

$$\partial_{k_y}\omega_r|_c = 0. \tag{A 24}$$

On the other hand, the real part of the frequency is found to depend on the value of k_x, so that:

$$\partial_{k_x}\omega_r|_c = Rc \neq 0, \tag{A 25}$$

which is consistent with the convective nature of LRs. The associated group velocity is found to depend linearly on the Reynolds number R, with the coefficient c in (2.9) given by

$$c = \tau^{-1}\int_{-1/2}^{1/2}\big[\big(k_c^{-2}V_1^2 + \big(W_1^2 + P\mathscr{R}_c^{(\pi/2)^{-1}}\Theta_1^2\big)\big)U_b - k_c^{-2}V_1 W_1\,\mathscr{D}U_p\big]\,\mathrm{d}z$$
$$\cong \tau^{-1}(0.4718 + 1.375P), \tag{A 26}$$

and

$$\tau = P^{-1}\int_{-1/2}^{1/2}\big[k_c^{-2}V_1^2 + \big(W_1^2 + P\mathscr{R}_c^{(\pi/2)^{-1}}\Theta_1^2\big)\big]\,\mathrm{d}z \cong P^{-1}(0.8012 + 1.566P). \tag{A 27}$$

A.4. *Solution of the second-order problem*

The solution $\boldsymbol{v}_2$ of (A 16) is sought in the form:

$$\boldsymbol{v}_2 = A^2\,\boldsymbol{V}_{2,2}(z)\exp(2\mathrm{i}k_c y_0) + \big(\partial_{\chi_1}A\,\boldsymbol{V}_{2,x}(z) + \partial_{y_1}A\,\boldsymbol{V}_{2,y}(z)\big)\exp(\mathrm{i}k_c y_0)$$
$$+ \tfrac{1}{2}A\overline{A}\boldsymbol{V}_{2,0}(z) + \tfrac{1}{2}\big[\tfrac{1}{2}\mathscr{R}_2 z(1-z),\ 0,\ 0,\ 0,\ \mathscr{R}_2\big(\tfrac{1}{2} - z\big)\big]^{\mathrm{T}} + \text{c.c.}, \tag{A 28}$$

where A depends on the variables χ_1, y_1 and t_2 which are related to t_1 and x_1 by

$$\partial_{t_1} = -R\,c\,\partial_{\chi_1}, \quad \partial_{x_1} = \partial_{\chi_1}. \tag{A 29}$$

In (A 28), $\boldsymbol{V}_{2,2}$ is the column vector

$$\boldsymbol{V}_{2,2} = \left[\left(2Pk_c^2\right)^{-1}\left(V_1^2 - W_1\mathscr{D}V_1\right) + P_{2,2},\ (2k_c)^{-2}RU_{2,2},\ \mathrm{i}k_c^{-1}V_{2,2},\ W_{2,2},\ \Theta_{2,2}\right]^{\mathrm{T}}, \tag{A 30}$$

and $\boldsymbol{V}_{2,0}$ is

$$\boldsymbol{V}_{2,0} = \left[P_{2,0},\ k_c^{-2}RU_{2,0},\ 0,\ 0,\ \Theta_{2,0}\right]^{\mathrm{T}}. \tag{A 31}$$

It then follows that $W_{2,2}$ and $\Theta_{2,2}$ satisfy

$$\left(\mathscr{D}^2 - 4k_c^2\right)^2 W_{2,2} - 4k_c^2\Theta_{2,2} = 2P^{-1}(W_1\,\mathscr{D}^3 W_1 - \mathscr{D}W_1\,\mathscr{D}^2 W_1), \tag{A 32a}$$

$$\left(\mathscr{D}^2 - 4k_c^2\right)\Theta_{2,2} - \mathscr{R}_c^{(\pi/2)}W_{2,2} = W_1\,\mathscr{D}\Theta_1 - \Theta_1\,\mathscr{D}W_1, \tag{A 32b}$$

and $\Theta_{2,0}$ satisfies

$$\mathscr{D}^2\Theta_{2,0} = 2\mathscr{D}(W_1\Theta_1), \tag{A 33}$$

which are similar to the equations in the absence of a mean through-flow. Consequently, the solutions are those given by Schlüter *et al.* (1965). This is also true for the remaining functions $V_{2,2}$, $V_{2,0}$, $P_{2,2}$, $P_{2,0}$. Furthermore, it is found that $U_{2,2}$ and $U_{2,0}$ do not provide resonant terms in the compatibility condition at third order, so that their determination is unnecessary.

Similarly, we define $\boldsymbol{V}_{2,x}$ as the column vector

$$\begin{aligned}\boldsymbol{V}_{2,x} = \big[&Rk_c^{-2}[(P^{-1}c - U_p)V_1 + W_1\,\mathscr{D}U_p + P_{2,x}],\ k_c^{-2}\left(V_1 + R^2k_c^{-2}U_{2,x}\right),\\ &\mathrm{i}Rk_c^{-3}(U_1 + V_{2,x}),\ Rk_c^{-2}W_{2,x},\ Rk_c^{-2}\Theta_{2,x}\big]^{\mathrm{T}}.\end{aligned} \tag{A 34}$$

The set of governing equations for $W_{2,x}$ and $\Theta_{2,x}$ is thus obtained as

$$\left(k_c^{-2}\mathscr{D}^2 - 1\right)^2 W_{2,x} - k_c^{-2}\Theta_{2,x} = (U_p - P^{-1}c)\left(k_c^{-2}\mathscr{D}^2 - 1\right)W_1 - k_c^{-2}W_1\,\mathscr{D}^2U_p, \tag{A 35a}$$

$$\left(k_c^{-2}\mathscr{D}^2 - 1\right)\Theta_{2,x} + k_c^{-2}\mathscr{R}_c^{(\pi/2)}W_{2,x} = P(U_p - P^{-1}c)\Theta_1, \tag{A 35b}$$

and the solution $W_{2,x}$ is found to be

$$W_{2,x} = \sum_{n=1}^{n=3} z(z^2G_{n,x} + H_{n,x})\sinh(q_nz) + (z^2I_{n,x} + C_{n,x})\cosh(q_nz). \tag{A 36}$$

Eliminating $\Theta_{2,x}$ in (A 35) allows us to determine the coefficients $G_{n,x}$, $H_{n,x}$ and $I_{n,x}$ as functions of C_n, q_n, k_c, P and c. They are, however, not listed here, as the expressions are too long. The $C_{n,x}$ terms, finally, are obtained by imposing the boundary conditions

$$W_{2,x}\left(\tfrac{1}{2}\right) = \Theta_{2,x}\left(\tfrac{1}{2}\right) = 0, \tag{A 37}$$

and the orthogonality condition

$$\sum_{n=1}^{n=3} C_nC_{n,x} = 0. \tag{A 38}$$

$\Theta_{2,x}$ is then obtained by relation (A 35a), and $V_{2,x}$ and $P_{2,x}$ by

$$V_{2,x} = \mathscr{D}W_{2,x}, \tag{A 39a}$$

$$P_{2,x} = \left(k_c^{-2}\mathscr{D}^2 - 1\right)V_{2,x}. \tag{A 39b}$$

Next the unknown function $U_{2,x}$ is governed by

$$\left(k_c^{-2}\mathscr{D}^2 - 1\right)U_{2,x} = W_{2,x}\,\mathscr{D}U_p + U_1(U_p - P^{-1}c), \tag{A 40}$$

and the solution $U_{2,x}$ may be written as

$$U_{2,x} = \sum_{n=1}^{n=3}[(J_{n,x}z^4 + K_{n,x}z^2 + L_{n,x})\sinh q_n z + z(M_{n,x}z^2 + N_{n,x})\cosh q_n z] + z(J_{0,x}z^2 + K_{0,x})\cosh k_c z + (L_{0,x} + D_{0,x})\sinh k_c z. \tag{A 41}$$

The coefficients in (A 41) are obtained by inserting (A 41) into (A 40) except for the coefficient $D_{0,x}$ which is obtained by imposing $U_{2,x}(\frac{1}{2}) = 0$.

Finally, we define $\boldsymbol{V}_{2,y}$ as the column vector

$$\boldsymbol{V}_{2,y} = 2\left[\mathrm{i}k_c^{-1}\left(k_c^{-2}\mathscr{D}^2 V_1 + P_{2,y}\right),\ \mathrm{i}Rk_c^{-3}U_{2,y},\ -k_c^{-2}(V_1/2 + V_{2,y}),\ \mathrm{i}k_c^{-1}W_{2,y},\ \mathrm{i}k_c^{-1}\Theta_{2,y}\right]^{\mathrm{T}}, \tag{A 42}$$

and the set of equations governing $W_{2,y}$ and $\Theta_{2,y}$ is given, as in the absence of a mean through-flow, by

$$\left(k_c^{-2}\mathscr{D}^2 - 1\right)^2 W_{2,y} - k_c^{-2}\Theta_{2,y} = -\left(k_c^{-4}\mathscr{D}^4 - 1\right)W_1, \tag{A 43a}$$

$$\left(k_c^{-2}\mathscr{D}^2 -\right)\Theta_{2,y} + k_c^{-2}\mathscr{R}_c^{(\pi/2)}W_2^{(y)} = -\Theta_1. \tag{A 43b}$$

The solution $W_{2,y}$ is sought in the form

$$W_{2,y} = \sum_{n=1}^{n=3} H_{n,y}z\sinh q_n z + C_{n,y}\cosh q_n z, \tag{A 44}$$

where the coefficients $H_{n,y}$ are obtained after eliminating $\Theta_{2,y}$ in (A 43), and $C_{n,y}$ is determined in the same way as $C_{n,x}$. $\Theta_{2,y}$ is then obtained from (A 43*a*) and $V_{2,y}$ and $P_{2,y}$ from

$$V_{2,y} = \mathscr{D}W_{2,y}, \tag{A 45a}$$

$$P_{2,y} = \left(k_c^{-2}\mathscr{D}^2 - 1\right)V_{2,y}. \tag{A 45b}$$

The remaining function $U_{2,y}$ satisfies:

$$\left(k_c^{-2}\mathscr{D}^2 - 1\right)U_{2,y} = W_{2,y}\,\mathscr{D}U_p - U_1. \tag{A 46}$$

It is sought in the form

$$U_{2,y} = \sum_{n=1}^{n=3}[(K_{n,y}z^2 + L_{n,y})\sinh q_n z + zN_{n,y}\cosh q_n z] + zK_{0,y}\cosh k_c z + D_{0,y}\sinh k_c z, \tag{A 47}$$

where the coefficients are obtained by inserting (A 47) into (A 46), except for $D_{0,y}$ which is obtained by imposing the boundary condition $U_{2,y}(\frac{1}{2}) = 0$.

A.5. *Third-order solvability condition*

At $O(\epsilon^3)$, the following non-homogeneous problem for $\boldsymbol{v}_3 = (p_3, \boldsymbol{u}_3, \theta_3)^{\mathrm{T}}$ is obtained

$$\mathscr{L}_0\boldsymbol{v}_3 = \mathscr{S}_3(\boldsymbol{v}_1,\ \boldsymbol{v}_2), \tag{A 48}$$

where $\mathscr{S}_3(\boldsymbol{v}_1,\ \boldsymbol{v}_2)$ is given by

$$\begin{aligned}\mathscr{S}_3(\boldsymbol{v}_1,\ \boldsymbol{v}_2) = \big[\nabla_1\cdot\boldsymbol{u}_2,\ -P^{-1}\big(\partial_{t_2}\boldsymbol{u}_1 + \boldsymbol{u}_1\cdot\nabla_0\boldsymbol{u}_2 + \boldsymbol{u}_2\cdot\nabla_0\boldsymbol{u}_1 + \boldsymbol{u}_1\cdot\nabla_1\boldsymbol{u}_1\big)\\ + R(P^{-1}c - U_p)\,\partial_{\chi_1}\boldsymbol{u}_2 - \nabla_1 p_2 + \nabla_1^2\boldsymbol{u}_1 + 2\partial_{y_1}\partial_{y_0}\boldsymbol{u}_2,\ -\partial_{t_2}\theta_1\\ - \boldsymbol{u}_1\cdot\nabla_0\theta_2 - \boldsymbol{u}_2\cdot\nabla_0\theta_1 - \boldsymbol{u}_1\cdot\nabla_1\theta_1 + RP(P^{-1}c - U_p)\,\partial_{\chi_1}\theta_2\\ +\nabla_1^2\theta_1 + 2\partial_{y_1}\partial_{y_0}\theta_2\big]^{\mathrm{T}},\end{aligned} \tag{A 49}$$

with ∇_1 now denoting

$$\nabla_1 = \big(\partial_{\chi_1},\ \partial_{y_1},\ 0\big)^{\mathrm{T}}. \tag{A 50}$$

Homogeneous boundary conditions are imposed at $z = \pm 1/2$ for $\boldsymbol{u}_3$ and θ_3.

The envelope equation (2.12) is obtained from the solvability condition:

$$\langle \mathscr{S}_3(\boldsymbol{v}_1,\ \boldsymbol{v}_2),\ \boldsymbol{v}_1^{\star}\rangle = 0. \tag{A 51}$$

The various coefficients in (2.12) are given by

$$\mu = \mathscr{R}_c^{(\pi/2)^{-1}} \int_{-1/2}^{1/2} W_1\Theta_1\,\mathrm{d}z, \tag{A 52a}$$

$$\xi = 4\int_{-1/2}^{1/2}\big[W_1(W_1 - W_{2,y}) + \mathscr{R}_c^{(\pi/2)^{-1}}\Theta_1(\Theta_1 - \Theta_{2,y}) - k_c^{-4}V_{2,y}\,\mathscr{D}^2V_1\big]\,\mathrm{d}z, \tag{A 52b}$$

$$\begin{aligned}\alpha = k_c^{-2}\int_{-1/2}^{1/2}[P^{-1}c - U_p]\big[k_c^{-2}V_1V_{2,x} + W_1W_{2,x} + P\mathscr{R}_c^{(\pi/2)^{-1}}\Theta_1\Theta_{2,x}\big]\,\mathrm{d}z\\ + k_c^{-4}\int_{-1/2}^{1/2} V_1W_{2,x}\,\mathscr{D}U_p\,\mathrm{d}z,\end{aligned} \tag{A 52c}$$

$$\begin{aligned}\eta = 2k_c^{-1}\int_{-1/2}^{1/2}[P^{-1}c - U_p]\big[k_c^{-2}V_1(V_1 + V_{2,y}) + W_1W_{2,y} + P\mathscr{R}_c^{(\pi/2)^{-1}}\Theta_1\Theta_{2,y}\big]\,\mathrm{d}z\\ + 2k_c^{-1}\int_{-1/2}^{1/2}\big[W_1W_{2,x} + \mathscr{R}_c^{(\pi/2)^{-1}}\Theta_1\Theta_{2,x} + k_c^{-4}V_{2,x}\,\mathscr{D}^2V_1\big]\,\mathrm{d}z\\ + 2k_c^{-3}\int_{-1/2}^{1/2} V_1[W_1 + W_{2,y}]\,\mathscr{D}U_p\,\mathrm{d}z.\end{aligned} \tag{A 52d}$$

Appendix B. The multiple scale analysis at infinitesimal R

B.1. *Reynolds number of* $O(\epsilon^{3/2})$

The successive problems at $O(\epsilon)$, $O(\epsilon^{3/2})$ and $O(\epsilon^2)$ are identical to those obtained in the absence of through-flow. Thus, $\boldsymbol{V}_{1,\varphi}$ in (3.4) is given by

$$\boldsymbol{V}_{1,\varphi} = \big(P_1,\ \mathrm{i}k_c^{-1}V_1,\ 0,\ W_1,\ \Theta_1\big)^{\mathrm{T}}, \tag{B 1}$$

with P_1, V_1, W_1 and Θ_1 as in Appendix A. The $O(\epsilon^{3/2})$ solution $\boldsymbol{v}_{3/2,\varphi}$ is obtained as

$$\boldsymbol{v}_{3/2,\varphi} = \partial_{y'_{1/2}}A_\varphi \exp\big(\big(\mathrm{i}k_c(x'_0 - R_{3/2}\,c\,\cos\varphi\,t_{3/2})\big)\big)\big[0,\ k_c^{-2}V_1\boldsymbol{e}_{y'},\ 0\big]^{\mathrm{T}} + \text{c. c.}, \tag{B 2}$$

and the $O(\epsilon^2)$ solution $\boldsymbol{v}_{2,\varphi}$ as

$$\begin{aligned}\boldsymbol{v}_{2,\varphi} = A_\varphi^2\,\boldsymbol{V}_{2,2,\varphi}(z)\exp\big(2\mathrm{i}k_c\big(x'_0 - R_{3/2}\,c\,\cos\varphi\,t_{3/2}\big)\big) + \big(2\mathrm{i}k_c^{-1}\partial_{x'_1}A_\varphi\,\boldsymbol{V}_{2,x',\varphi}(z)\\ + k_c^{-2}\partial^2_{y'_{1/2}}A_\varphi\,\boldsymbol{V}_{2,y',\varphi}(z)\big)\exp\big(\mathrm{i}k_c\big(x'_0 - R_{3/2}\,c\,\cos\varphi\,t_{3/2}\big)\big)\\ + \tfrac{1}{2}A_\varphi\overline{A_\varphi}\boldsymbol{V}_{2,0,\varphi}(z) + \tfrac{1}{2}\big[\tfrac{1}{2}\mathscr{R}_2 z(1-z),\ 0,\ 0,\ 0,\ \mathscr{R}_2\big(\tfrac{1}{2} - z\big)\big]^{\mathrm{T}} + \text{c. c.},\end{aligned} \tag{B 3}$$

where

$$\boldsymbol{V}_{2,2,\varphi} = \left[\left(2Pk_c^2\right)^{-1}\left(V_1^2 - W_1\mathscr{D}V_1\right) + P_{2,2},\ \mathrm{i}k_c^{-1}V_{2,2},\ 0,\ W_{2,2},\ \Theta_{2,2}\right]^{\mathrm{T}}, \tag{B 4a}$$

$$\boldsymbol{V}_{2,x',\varphi} = \left[k_c^{-2}\mathscr{D}^2V_1 + P_{2,y},\ \mathrm{i}k_c^{-1}(V_1/2 + V_{2,y}),\ 0,\ W_{2,y},\ \Theta_{2,y}\right]^{\mathrm{T}}, \tag{B 4b}$$

$$\boldsymbol{V}_{2,y',\varphi} = \left[k_c^{-2}\mathscr{D}^2V_1 + P_{2,y},\ \mathrm{i}k_c^{-1}(V_1 + V_{2,y}),\ 0,\ W_{2,y},\ \Theta_{2,y}\right]^{\mathrm{T}}, \tag{B 4c}$$

$$\boldsymbol{V}_{2,0,\varphi} = \left[P_{2,0},\ 0,\ 0,\ 0,\ \Theta_{2,0}\right]^{\mathrm{T}}, \tag{B 4d}$$

with all scalar functions of z as defined in Appendix A.

At $O(\epsilon^{5/2})$, $\boldsymbol{v}_{5/2,\varphi} = [p_{5/2,\varphi}, \boldsymbol{u}_{5/2,\varphi}, \theta_{5/2,\varphi}]^{\mathrm{T}}$ has to satisfy the following inhomogeneous linear problem

$$\mathscr{L}_{0,0}\boldsymbol{v}_{5/2,\varphi} = \mathscr{S}_{5/2}\left(\boldsymbol{v}_{1,\varphi}, \boldsymbol{v}_{3/2,\varphi}, \boldsymbol{v}_{2,\varphi}\right), \tag{B 5}$$

where $\mathscr{L}_{0,0}$ is the linear operator $\mathscr{L}_0$ evaluated at $R = 0$ and $\mathscr{S}_{5/2}(\boldsymbol{v}_{1,\varphi}, \boldsymbol{v}_{3/2,\varphi}, \boldsymbol{v}_{2,\varphi})$ is given by

$$\begin{aligned}\mathscr{S}_{5/2} = \big[0,\ &-P^{-1}\left(\partial_{t_{3/2}}\boldsymbol{u}_{1,\varphi} + \boldsymbol{u}_{1,\varphi}\cdot\nabla_0'\boldsymbol{u}_{3/2,\varphi}\right) - \partial_{y'_{1/2}}p_2\boldsymbol{e}_{y'} - R_{3/2}\,U_p\,\cos\varphi\,\partial_{x'_0}\boldsymbol{u}_{1,\varphi}\\ &- R_{3/2}\,\mathscr{D}U_p\,(\boldsymbol{u}_{1,\varphi}\cdot\boldsymbol{e}_z)\boldsymbol{e}_x + \left(2\partial_{x'_1}\partial_{x'_0} + \partial^2_{y'_{1/2}}\right)\boldsymbol{u}_{3/2,\varphi},\ -\partial_{t_{3/2}}\theta_{1,\varphi}\\ &- R_{3/2}P\,U_p\,\cos\varphi\,\partial_{x'_0}\theta_{1,\varphi}\big]^{\mathrm{T}},\end{aligned} \tag{B 6}$$

with

$$\nabla_0' = \left(\partial_{x'_0},\ 0,\ \partial_z\right)^{\mathrm{T}}. \tag{B 7}$$

The solvability condition of (B 5) leads to a non-trivial equation which yields the oscillatory behaviour of A_φ on the time scale $t_{3/2}$, with frequency given by equation (3.4). The solution $\boldsymbol{v}_{5/2,\varphi}$ is found to be

$$\begin{aligned}\boldsymbol{v}_{5/2,\varphi} = &-\mathrm{i}k_c^{-1}A_\varphi\partial_{y'_{1/2}}A_\varphi\,\boldsymbol{V}_{5/2,2,\varphi}(z)\exp\left(2\mathrm{i}k_c\left(x_0' - R_{3/2}\,c\,\cos\varphi\,t_{3/2}\right)\right)\\ &+\left(\mathrm{i}k_c^{-1}R_{3/2}A_\varphi\boldsymbol{V}_{5/2,x',\varphi}(z) + \left(2k_c^{-2}\partial_{x'_1}\partial_{y'_{1/2}}A_\varphi - \mathrm{i}k_c^{-3}\partial^3_{y'_{1/2}}A_\varphi\right)\boldsymbol{V}_{5/2,y',\varphi}(z)\right)\\ &\times\exp\left(\mathrm{i}k_c\left(x_0' - R_{3/2}\,c\,\cos\varphi\,t_{3/2}\right)\right)\\ &+\overline{A}_\varphi\partial_{y'_{1/2}}A_\varphi\,\boldsymbol{V}_{5/2,0,\varphi}(z) + \tfrac{1}{48}\,\partial_{y'_{1/2}}\mathscr{R}_2\left(\tfrac{1}{4} - z^2\right)\left(\tfrac{1}{2}z^2 - z + \tfrac{1}{8}\right) + \text{c. c.},\end{aligned} \tag{B 8}$$

where

$$\boldsymbol{V}_{5/2,2,\varphi} = \left[0,\ 0,\ \mathrm{i}k_c^{-1}V_{2,2},\ 0,\ 0\right]^{\mathrm{T}}, \tag{B 9a}$$

$$\begin{aligned}\boldsymbol{V}_{5/2,x',\varphi} = \big[&(P^{-1}c - U_p)V_1 + W_1\,\mathscr{D}U_p + P_{2,x})\cos\varphi,\ \mathrm{i}k_c^{-1}V_{2,x}\cos\varphi,\\ &\mathrm{i}k_c^{-1}U_1\sin\varphi,\ W_{2,x}\cos\varphi,\ \Theta_{2,x}\cos\varphi\big]^{\mathrm{T}},\end{aligned} \tag{B 9b}$$

$$\boldsymbol{V}_{5/2,y',\varphi} = \left[0,\ 0,\ \mathrm{i}k_c^{-1}(V_1 + V_{2,y}),\ 0,\ 0\right]^{\mathrm{T}}. \tag{B 9c}$$

The determination of $\boldsymbol{V}_{5/2,0,\varphi}$ is not necessary for the present purpose.

Finally, at $O(\epsilon^3)$, the inhomogeneous linear problem to be solved is

$$\mathscr{L}_{0,0}\boldsymbol{v}_{3,\varphi} = \mathscr{S}_3\left(\boldsymbol{v}_{1,\varphi}, \boldsymbol{v}_{3/2,\varphi}, \boldsymbol{v}_{2,\varphi}, \boldsymbol{v}_{5/2,\varphi}\right), \tag{B 10}$$

where $\mathscr{S}_3(\boldsymbol{v}_{1,\varphi}, \boldsymbol{v}_{3/2,\varphi}, \boldsymbol{v}_{2,\varphi}, \boldsymbol{v}_{5/2,\varphi})$ is given by

$$\begin{aligned}\mathscr{S}_3 = \big[&\partial_{x'_1}(\boldsymbol{u}_{2,\varphi}\cdot\boldsymbol{e}_{x'}) + \partial_{y'_{1/2}}(\boldsymbol{u}_{5/2,\varphi}\cdot\boldsymbol{e}_{y'}),\ -P^{-1}\big\{\partial_{t_2}\boldsymbol{u}_{1,\varphi} + \partial_{t_{3/2}}\boldsymbol{u}_{3/2,\varphi} + \boldsymbol{u}_{2,\varphi}\cdot\nabla_0'\boldsymbol{u}_{1,\varphi}\\ &+\boldsymbol{u}_{1,\varphi}\cdot\nabla_0'\boldsymbol{u}_{2,\varphi} + (\boldsymbol{u}_{1,\varphi}\cdot\boldsymbol{e}_{x'})\,\partial_{x'_1}\boldsymbol{u}_{1,\varphi} + \left(\boldsymbol{u}_{3/2,\varphi}\cdot\boldsymbol{e}_{y'}\right)\partial_{y'_{1/2}}\boldsymbol{u}_{1,\varphi}\big\} - \partial_{x'_{1/2}}p_{2,\varphi}\boldsymbol{e}_{x'}\\ &-\partial_{y'_{1/2}}p_{5/2,\varphi}\boldsymbol{e}_{y'} - R_{3/2}\,U_p\,\cos\varphi\,\partial_{x'_0}\boldsymbol{u}_{3/2,\varphi} + R_{3/2}\,U_p\,\sin\varphi\,\partial_{y'_{1/2}}\boldsymbol{u}_{2,\varphi} + \partial^2_{x'_1}\boldsymbol{u}_{1,\varphi}\end{aligned}$$

$$+\left(2\partial_{x_1'}\partial_{x_0'}+\partial^2_{y'_{1/2}}\right)\boldsymbol{u}_{3/2,\varphi},\ -\partial_{t_2}\theta_{1,\varphi}-\boldsymbol{u}_{2,\varphi}\cdot\nabla_0'\theta_{1,\varphi}-\boldsymbol{u}_{1,\varphi}\cdot\nabla_0'\theta_{2,\varphi}$$
$$-(\boldsymbol{u}_{1,\varphi}\cdot\boldsymbol{e}_{x'})\,\partial_{x_1'}\theta_{1,\varphi}-\left(\boldsymbol{u}_{3/2,\varphi}\cdot\boldsymbol{e}_{y'}\right)\partial_{y'_{1/2}}\theta_{1,\varphi}-R_{3/2}P\,U_p\,\sin\varphi\,\partial_{y'_{1/2}}\theta_{1,\varphi}$$
$$+\partial^2_{x'_1}\theta_{1,\varphi}+\left(2\partial_{x_1'}\partial_{x_0'}+\partial^2_{y'_{1/2}}\right)\theta_{2,\varphi}\big]^{\mathrm{T}}. \tag{B 11}$$

The solvability condition for (B 10) then leads to the envelope equation (3.5).

B.2. *Reynolds number of* $O(\epsilon)$

For $R=O(\epsilon)$, the problems at $O(\epsilon)$ and $O(\epsilon^3/2)$ remain identical to those given in Appendix B.1. At $O(\epsilon^2)$, however, the solution $\boldsymbol{v}'_{2,\varphi}$ must be modified to include Reynolds-dependent terms:

$$\boldsymbol{v}'_{2,\varphi}=\boldsymbol{v}_{2,\varphi}+\mathrm{i}k_c^{-1}R_1A_\varphi\boldsymbol{V}_{5/2,x',\varphi}(z)\exp(\mathrm{i}k_c(x_0'-R_1\,c\,\cos\varphi\,t_1)), \tag{B 12}$$

where the same notation is used as in the previous section. At $O(\epsilon^{5/2})$, the right-hand side of the linear, inhomogeneous problem for $\boldsymbol{v}'_{5/2,\varphi}$ becomes

$$\mathscr{S}'_{5/2}=\big[\partial_{y'_{1/2}}(\boldsymbol{u}'_{2,\varphi}\cdot\boldsymbol{e}_{y'}),\ -P^{-1}\left(\partial_{t_{3/2}}\boldsymbol{u}'_{1,\varphi}+\boldsymbol{u}'_{1,\varphi}\cdot\nabla_0'\boldsymbol{u}'_{3/2,\varphi}+\partial_{t_1}\boldsymbol{u}'_{3/2,\varphi}\right)-\partial_{y'_{1/2}}p'_2\boldsymbol{e}_{y'}$$
$$+R_1\,U_p\,\sin\varphi\,\partial_{y'_{1/2}}\boldsymbol{u}'_{1,\varphi}-R_1\,U_p\cos\varphi\,\partial_{x_0'}\boldsymbol{u}'_{3/2,\varphi}+\left(2\partial^2_{x_1'}\partial_{x_0'}+\partial^2_{y'^2_{1/2}}\right)\boldsymbol{u}'_{3/2,\varphi},$$
$$-\partial_{t_{3/2}}\theta'_{1,\varphi}+R_1P\,U_p\,\sin\varphi\,\partial_{y'_{1/2}}\theta'_{1,\varphi}\big]^{\mathrm{T}}. \tag{B 13}$$

The solvability condition yields the following equation for the envelope A_φ

$$\partial_{t_{3/2}}A_\varphi=R_1\,c\,\sin\varphi\,\partial_{y'_{1/2}}A_\varphi, \tag{B 14}$$

with its solution given by (3.16). Then, $\boldsymbol{v}'_{5/2,\varphi}$ is found as

$$\boldsymbol{v}'_{5/2,\varphi}=-\mathrm{i}k_c^{-1}A_\varphi\partial_{\upsilon'_{1/2}}A_\varphi\,\boldsymbol{V}_{5/2,2,\varphi}(z)\exp(2\mathrm{i}k_c(x_0'-R_1\,c\,\cos\varphi\,t_1))$$
$$+k_c^{-2}\big(-R_1\,\boldsymbol{V}'_{5/2,x',\varphi}(z)+\left(2\partial_{x_1'}-\mathrm{i}k_c^{-1}\partial^2_{\upsilon'_{1/2}}\right)\boldsymbol{V}_{5/2,y',\varphi}(z)\big)\partial_{\upsilon'_{1/2}}A_\varphi$$
$$\times\exp(\mathrm{i}k_c(x_0'-R_1\,c\,\cos\varphi\,t_1))+\overline{A}_\varphi\partial_{\upsilon'_{1/2}}A_\varphi\,\boldsymbol{V}_{5/2,0,\varphi}(z)$$
$$+\tfrac{1}{48}\,\partial_{\upsilon'_{1/2}}\mathscr{R}_2\left(\tfrac{1}{4}-z^2\right)\left(\tfrac{1}{2}z^2-z+\tfrac{1}{8}\right)+\text{c. c.}, \tag{B 15}$$

with

$$\boldsymbol{V}'_{5/2,x',\varphi}=\big[(P^{-1}c-U_p)V_1+W_1\,\mathscr{D}U_p+P_{2,x})\sin\varphi,\ \mathrm{i}k_c^{-1}(V_{2,x}+U_1)\sin\varphi,$$
$$-\mathrm{i}k_c^{-1}(V_{2,x}+U_1)\cos\varphi,\ W_{2,x}\sin\varphi,\ \Theta_{2,x}\sin\varphi\big]^{\mathrm{T}}. \tag{B 16}$$

Finally, at $O(\epsilon^3)$, the right-hand side of the linear, inhomogeneous problem is

$$\mathscr{S}'_3=\big[\partial_{x_1'}(\boldsymbol{u}'_{2,\varphi}\cdot\boldsymbol{e}_{x'})+\partial_{\upsilon'_{1/2}}\left(\boldsymbol{u}'_{5/2,\varphi}\cdot\boldsymbol{e}_{y'}\right),\ -P^{-1}\big\{\partial_{t_2}\boldsymbol{u}'_{1,\varphi}+\partial_{t_1}\boldsymbol{u}'_{2,\varphi}+\boldsymbol{u}'_{2,\varphi}\cdot\nabla_0'\boldsymbol{u}'_{1,\varphi}$$
$$+\boldsymbol{u}'_{1,\varphi}\cdot\nabla_0'\boldsymbol{u}'_{2,\varphi}+\left(\boldsymbol{u}'_{1,\varphi}\cdot\boldsymbol{e}_{x'}\right)\partial_{x_1'}\boldsymbol{u}'_{1,\varphi}+\left(\boldsymbol{u}'_{3/2,\varphi}\cdot\boldsymbol{e}_{y'}\right)\partial_{\upsilon'_{1/2}}\boldsymbol{u}'_{1,\varphi}\big\}-\partial_{x_1'}p'_{2,\varphi}\,\boldsymbol{e}_{x'}$$
$$-\partial_{\upsilon'_{1/2}}p'_{5/2,\varphi}\,\boldsymbol{e}_{y'}-R_1(P^{-1}c-U_p)\sin\varphi\,\partial_{\upsilon'_{3/2}}\boldsymbol{u}'_{3/2,\varphi}-R_1\,U_p\,\cos\varphi\,\left(\partial_{x_0'}\boldsymbol{u}'_{2,\varphi}\right.$$
$$\left.+\partial_{x_1'}\boldsymbol{u}'_{1,\varphi}\right)+R_1\,\mathscr{D}U_p\,(\boldsymbol{u}'_{2,\varphi}\cdot\boldsymbol{e}_z)\boldsymbol{e}_x+\partial^2_{x'_1}\boldsymbol{u}'_{1,\varphi}+\left(2\partial_{x_1'}\partial_{x_0'}+\partial^2_{\upsilon'_{1/2}}\right)\boldsymbol{u}'_{3/2,\varphi},$$
$$-\partial_{t_2}\theta'_{1,\varphi}-\partial_{t_1}\theta'_{2,\varphi}-\boldsymbol{u}'_{2,\varphi}\cdot\nabla_0'\theta'_{1,\varphi}-\boldsymbol{u}'_{1,\varphi}\cdot\nabla_0'\theta'_{2,\varphi}-(\boldsymbol{u}'_{1,\varphi}\cdot\boldsymbol{e}_{x'})\,\partial_{x_1'}\theta'_{1,\varphi}$$
$$-\left(\boldsymbol{u}'_{3/2,\varphi}\cdot\boldsymbol{e}_{y'}\right)\partial_{\upsilon'_{1/2}}\theta'_{1,\varphi}-R_1P\,U_p\,\cos\varphi\,\left(\partial_{x_1'}\theta'_{1,\varphi}+\partial_{x_0'}\theta'_{2,\varphi}\right)+\partial^2_{x'_1}\theta'_{1,\varphi}$$
$$+\left(2\partial_{x_1'}\partial_{x_0'}+\partial^2_{\upsilon'_{1/2}}\right)\theta'_{2,\varphi}\big]^{\mathrm{T}}, \tag{B 17}$$

from which the envelope equation (3.17) is deduced.

REFERENCES

Akiyama, M., Hwang, G. J. & Cheng, K. C. 1971 Experiments on the onset of longitudinal vortices in laminar forced convection between horizontal plates. *J. Heat Transfer* **93**, 335–341.

Bénard, H. 1900 Tourbillons cellulaires dans une nappe liquide. *Rev. gén. Sci. pur. appl.* **11**, 1261–1271, 1309–1328.

Brevdo, L. 1991 Three-dimensional absolute and convective instabilities, and spatially amplifying waves in parallel shear flows. *Z. Angew. Math. Phys.* **42**, 911–942.

Briggs, R. J. 1964 *Electron-Stream Interaction With Plasmas*. MIT Press, Cambridge, MA.

Carrière, P. & Monkewitz, P. A. 1999 Convective versus absolute instability in mixed Rayleigh–Bénard–Poiseuille convection. *J. Fluid Mech.* **384**, 243–262.

Carrière, P. & Monkewitz, P. A. 2001 Transverse-roll global modes in a Rayleigh–Bénard–Poiseuille system with streamwise variable heating. *Eur. J. Mech.* B/*Fluids* **20**, 751–770.

Champeney, D. C. 1973 *Fourier Transforms and their Physical Applications*. Academic.

Chang, M. Y., Yu, C. H. & Lin, T. F. 1997 Flow visualization and numerical simulation of transverse and mixed vortex roll formation in mixed convection of air in a horizontal flat duct. *Intl J. Heat Mass Transfer* **40**, 1907–1922.

Chen, S. S. & Lavine, A. S. 1996 Laminar, buoyancy induced flow structures in a bottom heated, aspect ratio 2 duct with throughflow. *Intl J. Heat Mass Transfer* **39**, 1–11.

Fujimura, K. & Kelly, R. E. 1995 Interaction between longitudinal convection rolls and transverse waves in unstably stratified plane Poiseuille flow. *Phys. Fluids* **7**, 68–79.

Fukui, K., Nakajima, M. & Hueda, H. 1983 The longitudinal vortex and its effects on the transport processes in combined free and forced laminar convection between horizontal and inclined parallel plates. *Intl J. Heat Mass Transfer* **26**, 109–120.

Gage, K. S. & Reid, W. H. 1968 The stability of thermally stratified plane Poiseuille flow. *J. Fluid Mech.* **33**, 21–32.

Joseph, D. D. 1976 *Stability of Fluid Motions*. Springer.

Kelly, R. E. 1994 The onset and development of thermal convection in fully developed shear flows. *Adv. Appl. Mech.* **31**, 35–112.

Koschmieder, E. L. & Pallas, S. G. 1974 Heat transfer through a shallow, horizontal convecting fluid layer. *Intl J. heat Mass Transfer* **17**, 991–1002.

Landau, L. 1944 On the problem of turbulence. In *Collected Papers of L. D. Landau*, p. 387. Gordon and Breach, New York.

Luijkx, J. M., Platten, J. K. & Legros, J.-C. 1981 On the existence of thermoconvective rolls, transverse to a superimposed mean Poiseuille flow. *Intl J. Heat Mass Transfer* **24**, 1287–1291.

Malkus, W. V. R. & Veronis, G. 1958 Finite amplitude cellular convection. *J. Fluid Mech.* **4**, 225–260.

Martinand, D., Carrière, Ph. & Monkewitz, P. A. 2004 Envelope equation for the Raleigh–Bénard–Poiseuille system. Part 2. Linear global modes in the case of two-dimensional non-uniform heating. *J. Fluid Mech.* **502**, 175–197.

Müller, H. W. 1990 Thermische Konvektion in Horizontaler Scherströmung. PhD thesis, Universität des Saarlandes, Saarbrüken.

Müller, H. W., Lücke, M. & Kamps, M. 1992 Transversal convection patterns in horizontal shear flow. *Phys. Rev.* A **45**, 3714–3726.

Newell, A. C. & Whitehead, J. A. 1969 Finite bandwidth, finite amplitude convection. *J. Fluid Mech.* **38**, 279–303.

Ostrach, S. & Kamotani, Y. 1975 Heat transfer augmentation in laminar fully developed channel flow by means of heating from below. *J. Heat Transfer* **97**, 220–225.

Ouazzani, M. T., Catalgirone, J. P., Meyer, G. & Mojtabi, A. 1989 Etude numérique et expérimentale de la convection mixte entre deux plans horizontaux à températures différentes. *Intl J. Heat Mass Transfer* **32**, 261–269.

Ouazzani, M. T., Platten, J. K. & Mojtabi, A. 1990 Etude numérique et expérimentale de la convection mixte entre deux plans horizontaux à températures différentes–II. *Intl J. Heat Mass Transfer* **33**, 1417–1427.

Ouazzani, M. T., Platten, J. K., Müller, H. W. & Lücke, M. 1995 Etude de la convection mixte entre deux plans horizontaux à température différentes–III. *Intl J. Heat Mass Transfer* **38**, 875–886.

Palm, E. 1960 On the tendency towards hexagonal cells in steady convection. *J. Fluid Mech.* **38**, 183–192.

Pellew, A. & Southwell, R. V. 1940 On maintained convective motion in a fluid heated from below. *Proc. R. Soc.* A **176**, 312–343.

Rayleigh, L. 1916 On convection currents in a horizontal layer of fluid when the higher temperature is on the under side. *Phil. Mag.* **32**, 529–546.

Richter, F. M. 1973 Convection and the large scale circulation of the mantle. *Geophys. Res.* **78**, 8735–8745.

Schlüter, A., Lortz, D. & Busse, F. H. 1965 On the stability of steady finite amplitude convection. *J. Fluid Mech.* **23**, 129–144.

Schröder, E. & Bühler, K. 1995 Three-dimensional convection in rectangular domains with horizontal throughflow. *Intl J. Heat Mass Transfer* **38**, 1249–1259.

Segel, L. A. 1969 Distant side-walls cause slow amplitude modulation of cellular convection. *J. Fluid Mech.* **38**, 203–224.

Silveston, P. L. 1958 Aärmedurchgang in waagerechten flüssigkeitsschichten. *Forsch. Ingenieurwes.* **24**, 29–32, 59–69.

Sorokin, V. S. 1953 Variational method in the theory of convection. *Prikl. Mat. Mekh.* **17**, 39.

Sorokin, V. S. 1954 Stationary motions in a fluid heated from below. *Prikl. Mat. Mekh.* **18**, 197.

Stewartson, K. & Stuart, J. T. 1971 A non-linear instability theory for a wave system in plane Poiseuille flow. *J. Fluid Mech.* **48**, 529–545.

Stuart, J. T. 1960 Non-linear mechanics of disturbances in parallel flows. Part 1. *J. Fluid Mech.* **9**, 353–370.

Walton, I. C. 1985 The effect of a shear flow on convection in a layer heated non-uniformly from below. *J. Fluid Mech.* **154**, 303–319.

White, D. B. 1988 The planforms and onset of convection with a temperature-dependent viscosity. *J. Fluid Mech.* **191**, 247–286.

Yu, C. H., Chang, M. Y., Huang, C. C. & Lin, T. F. 1997 Structures of moving transverse and mixed rolls in mixed convection of air in a horizontal plane channel. *Intl J. Heat Mass Transfer* **40**, 333–346.